

Supplemental data related to the manuscript

**Structural basis for RNA-genome recognition during bacteriophage  
Q $\beta$  replication**

Heidi Gytz, Durita Mohr, Paulina Seweryn, Yuichi Yoshimura, Zarina Kutlubaeva,  
Fleur Dolman, Bosene Chelchessa, Alexander B. Chetverin, Frans A. A. Mulder,  
Ditlev E. Brodersen and Charlotte R. Knudsen

## Supplemental Figure legends

**Figure S1. Analysis of molecular weights and elution volumes of monomeric and dimeric forms of the Q $\beta$  replicase core complex.** Molecular weights and elution volumes were analysed after gel filtration over a Superdex 200 10/300 GL column coupled to static light scattering equipment. Gel filtration profile of monomeric (**A**) and dimeric (**B**) Q $\beta$  replicase core complex.

**Figure S2. Representative example of the electron density map.** The N-terminal  $\alpha$ -helix of OB<sub>1</sub> is shown as a purple cartoon with side chains as sticks, while the rest of the structure is coloured as denoted in figure 3. The final, refined 2mFo-DFc  $\sigma$ -A weighted map is depicted as a black mesh contoured at 1.0  $\sigma$ .

**Figure S3. Interaction of the OB<sub>1-2</sub> domains of ribosomal protein S1 with the  $\beta$ -subunit of the Q $\beta$  replicase complex.** **A.** OB<sub>1-2</sub> (in magenta) interacts with the fingers domain (green) of the  $\beta$ -subunit. Other subdomains are the palm domain in cyan and the thumb domain in pale pink. The active site residues Asp274, Asp359 and Asp360 are shown as red spheres. The RNA product and template strands are docked by superpositioning with the RNA-bound Q $\beta$  replicase core complex (PDB ID 3AVY). **B.** Zoom-in on details of the interaction between OB<sub>1-2</sub> and the  $\beta$ -subunit. In the following text, residues in the  $\beta$ -subunit, EF-Tu and S1 are indicated with the prefixes  $\beta$ , u and s, respectively. Panel a. The  $\beta$ -barrel of OB<sub>1</sub> forms two salt bridges to the  $\beta$ -subunit that define the outer boundary of the interface, sLys43 to  $\beta$ Asp202 and sAsp39 to  $\beta$ Arg191 and  $\beta$ Arg199. The bottom of the barrel is packed against residues 181-203 of the  $\beta$ -subunit via hydrophobic interactions. Panel b. The N-terminal helix of OB<sub>1</sub> engages in  $\pi$ -stacking interactions as follows: sPhe5–uPhe261, sPhe9– $\beta$ Leu149 and sLeu13– $\beta$ Tyr186. Furthermore, sIle16 and  $\beta$ Leu188 form a van der Waals interaction and a hydrogen bond is present between sSer12 and  $\beta$ Ala189. Salt bridges between sThr2 and uArg262 as well as sGlu17 and  $\beta$ Lys185 stabilizes the N and C-terminal end of the helix, respectively. Panel c. The  $\alpha$ -helix of the linker connecting OB domains 1 and 2 (residues 87-102) contributes to the binding of OB<sub>2</sub> to the  $\beta$ -subunit via a salt bridge between  $\beta$ Glu288 and sArg91 as well as hydrogen bonds between the backbone of  $\beta$ Ala104 and sArg86. Further interactions between

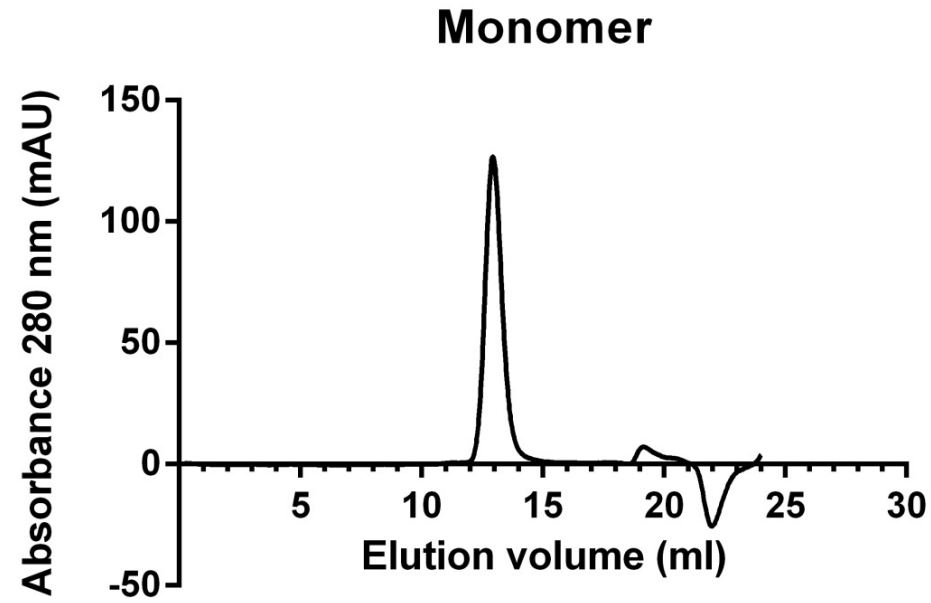
the  $\beta$ -subunit and OB<sub>2</sub> are as follows: sArg128 interacts with both  $\beta$ Glu125 and the main chain of  $\beta$ Leu110, sGlu123 and sAsn113 interact with  $\beta$ Tyr115, sAsn165 interacts with  $\beta$ Arg132, sVal116 and sThr121 stacks with  $\beta$ His129, sArg163 interacts with  $\beta$ Asp141 and lastly, sAsn125 interacts with  $\beta$ Arg112. Only a part of the mentioned interactions is shown in the figure for clarity.

**Figure S4. Crystallographic dimers of Q $\beta$  replicase complexes.** The crystallographic dimers of the Q $\beta$  replicase core complex (PDB ID 3MMP; upper panel), the OB<sub>1-2</sub>-bound Q $\beta$  replicase complex (this study; middle panel) and the Q $\beta$  replicase core complex crystallized with OB<sub>1-3</sub> (PDB ID 4Q7J; lower panel) are presented from two different views (left and right, respectively). The darker coloured monomers are presented in identical views, whereas the lighter coloured monomers are positioned relative to their dimer counterpart. Orange:  $\beta$ -subunit, purple: OB domains, blue: EF-Tu and green: EF-Ts.

**Figure S5. Structural changes occurring in the Q $\beta$  replicase core complex upon binding of the OB<sub>1-2</sub> or OB<sub>1-3</sub> protein.** The  $\beta$ -subunits of the unbound (turquoise, PDB ID 3MMP), RNA-bound (grey, PDB ID 3AVY), OB<sub>1-2</sub> bound (yellow, this study) and OB<sub>1-3</sub> bound (purple, PDB ID 4Q7J) Q $\beta$  replicase core complexes were superimposed. The arrow indicates a rotation of the EF-Tu-EF-Ts subcomplex towards the cavity forming the RNA exit channel. The largest displacement caused by this rotation is found in EF-Ts in which helices are displaced by up to 9.4 Å (OB<sub>1-3</sub> bound complex). The displacement of a flexible loop in the  $\beta$ -subunit caused by OB<sub>1-2</sub> binding is enlarged for clarity. Major distance changes are indicated.

**Figure S6. The N-terminal  $\alpha$ -helix of S1.** Presentation of the helix-binding site on the Q $\beta$  replicase core complex and the ribosome, same view in all. **A.** Binding of the PEP compound (green) in the Q $\beta$  replicase core complex (PDB ID 3MMP). The  $\beta$ -subunit is coloured orange and EF-Tu is coloured blue. The PEP compound binds the same hydrophobic groove on the Q $\beta$  replicase core complex as the N-terminal helix. **B.** Binding of the N-terminal helix of OB<sub>1</sub> (purple) in the on the Q $\beta$  replicase core complex. **C.** Binding of the N-terminal helix of OB<sub>1</sub> (purple) to the ribosomal protein S2 (green) (PDB ID 4TOI).

A



B

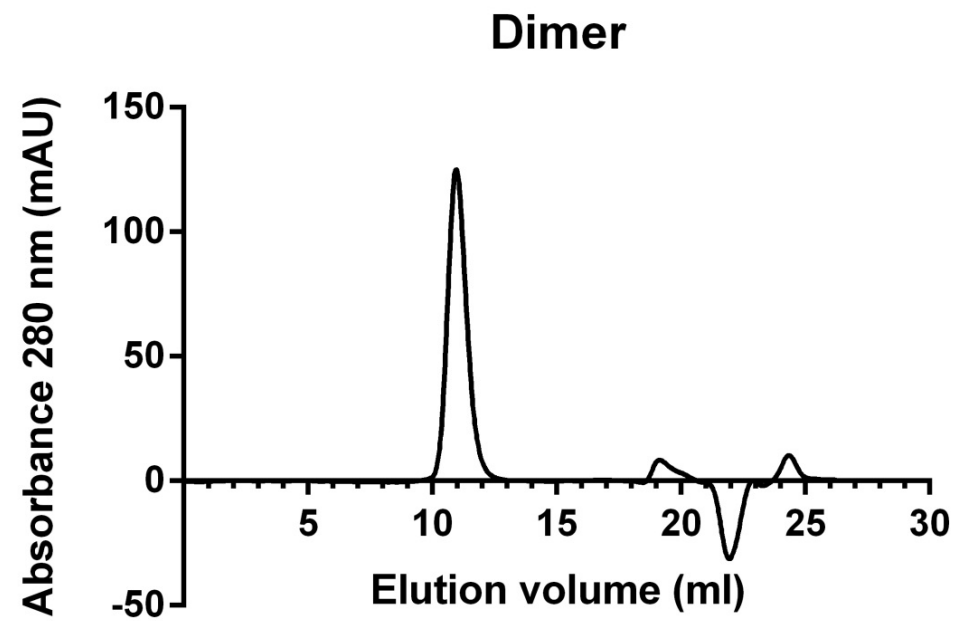


Figure S1

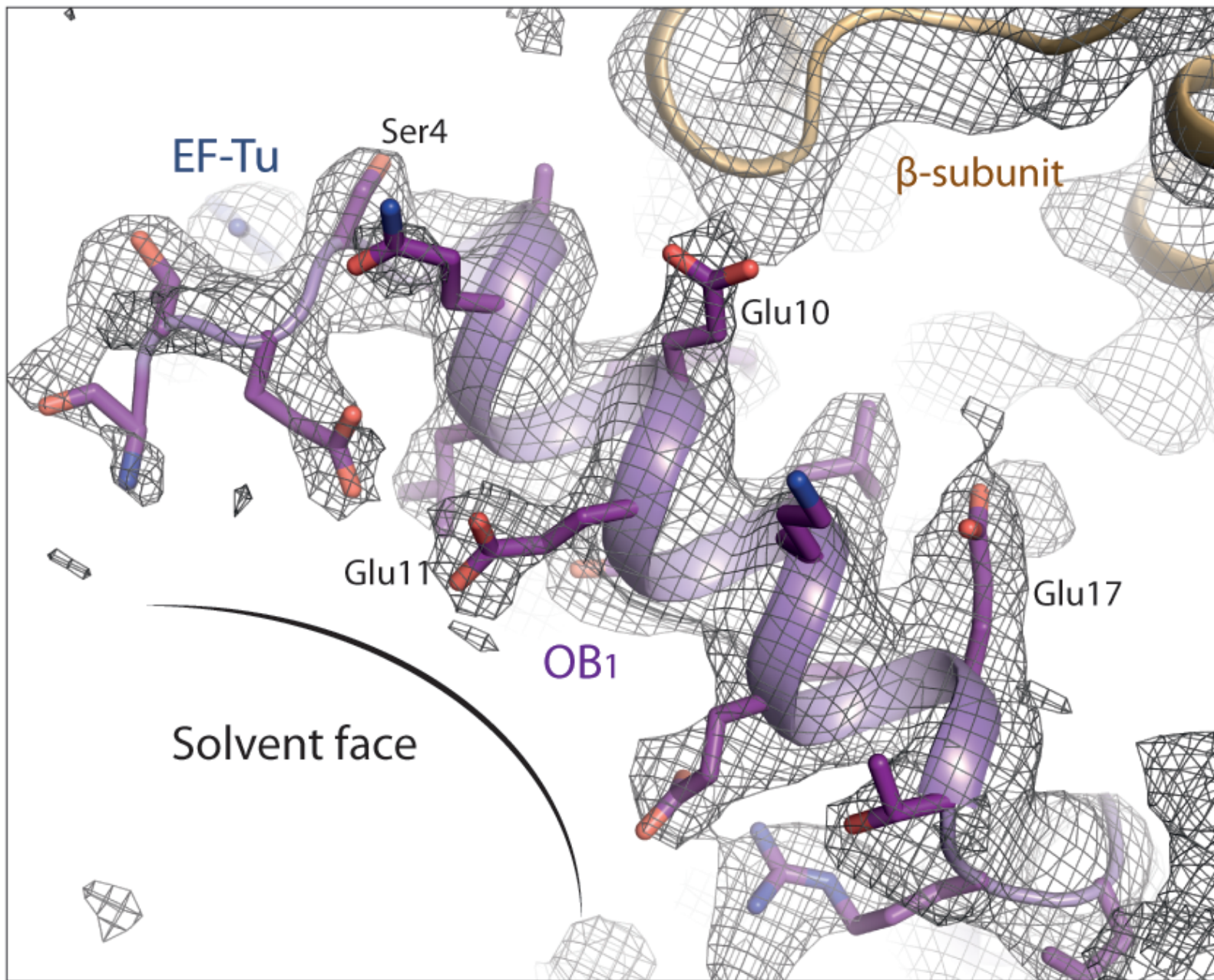


Figure S2

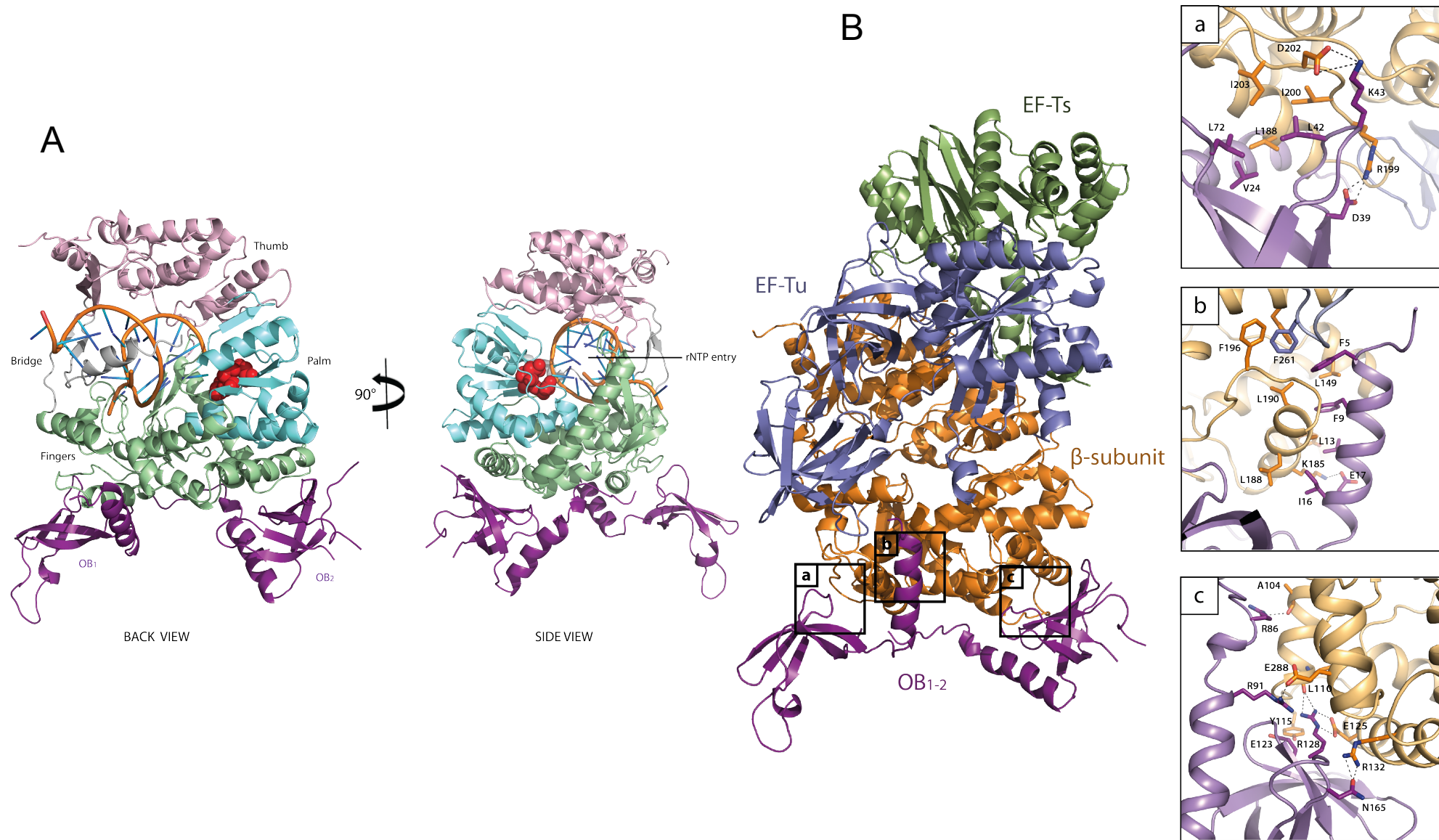


Figure S3

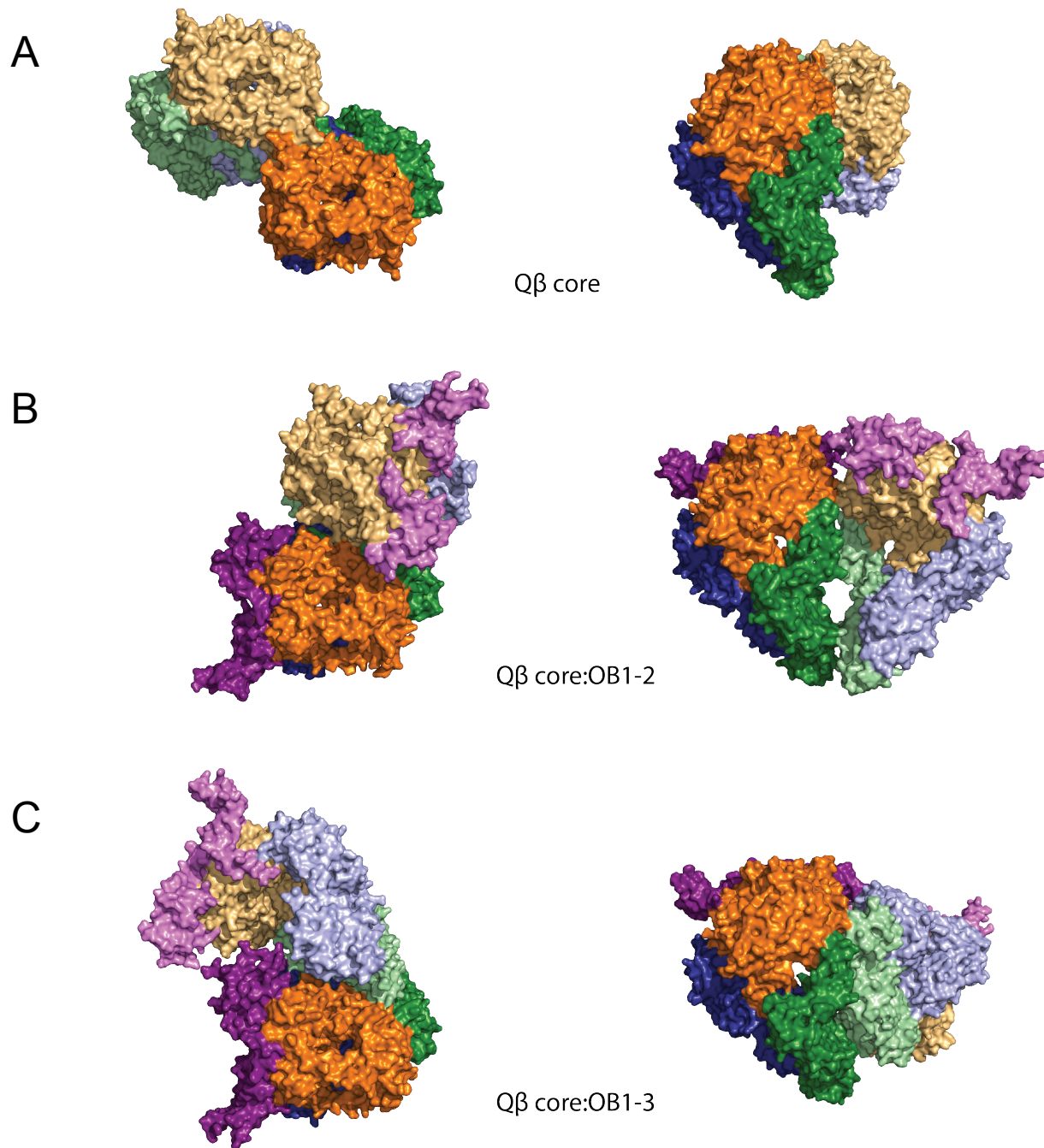


Figure S4

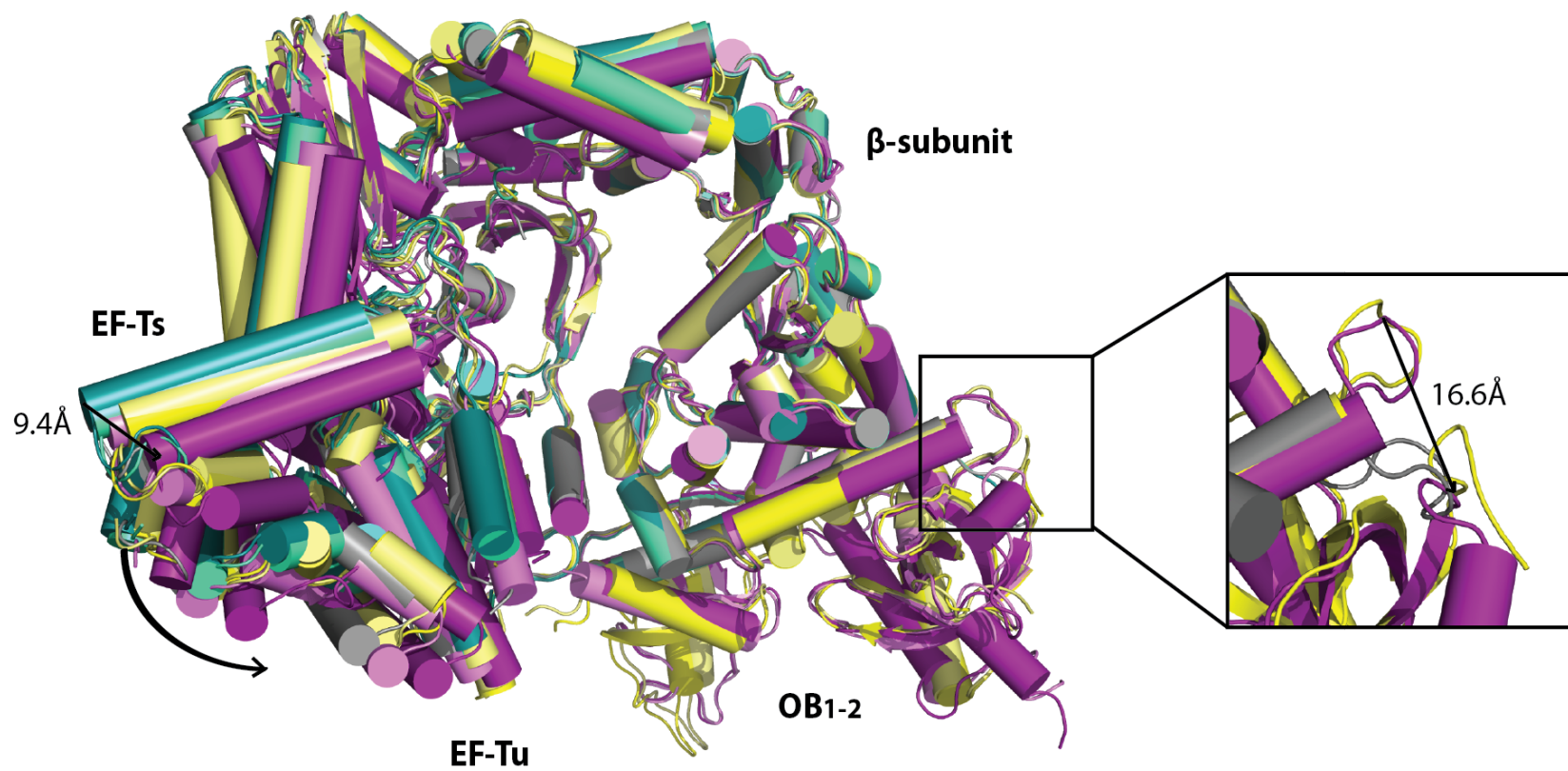


Figure S5



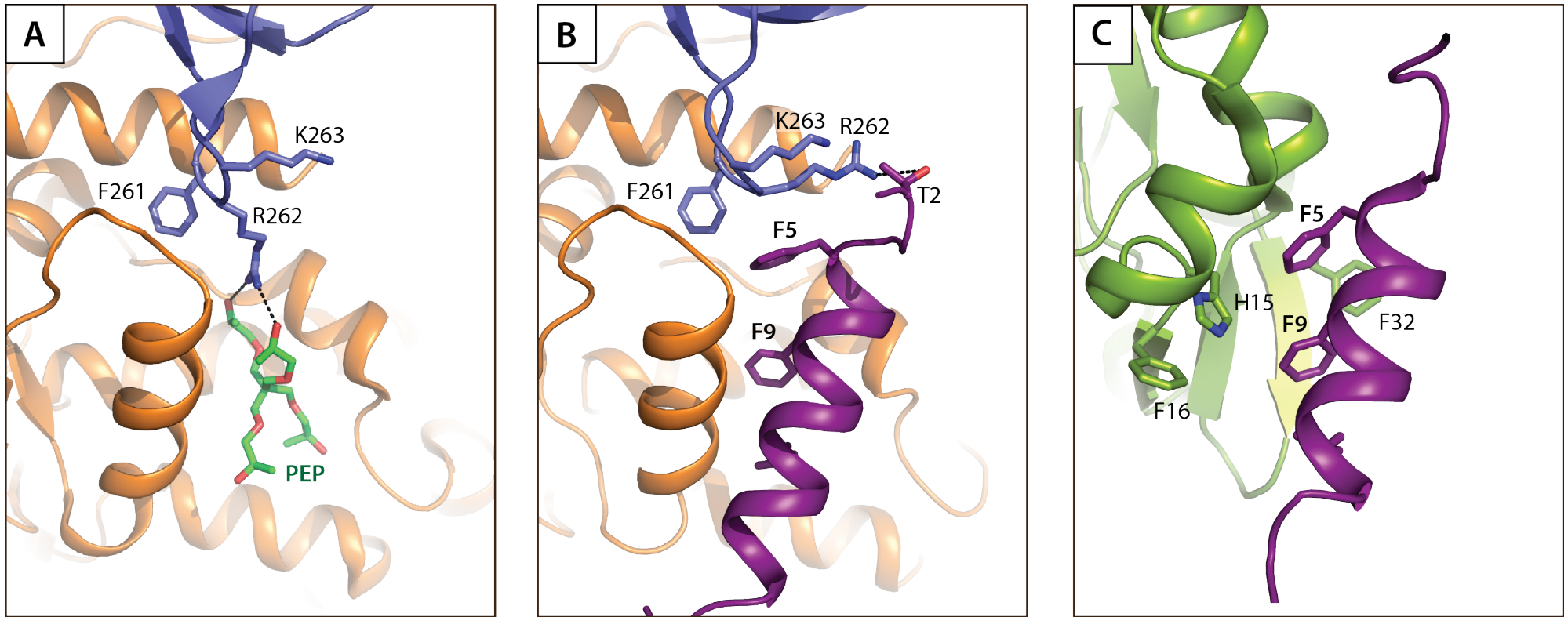


Figure S6